



Gradu Amaierako Lana / Trabajo Fin de Grado  
Biokimika eta Biologia Molekularreko Gradua / Grado en Bioquímica y Biología Molecular

# Transcriptional deregulation of cell cycle by PGC1 $\alpha$ in prostate cancer

Egilea/Autor/a:  
Aintzane Rodríguez Barrante  
Zuzendaria/Director/a:  
Verónica Torrano Moya

# CONTENTS

<b>1. INTRODUCTION</b> .....	<b>1</b>
<b>2. HYPOTHESIS AND OBJECTIVES</b> .....	<b>3</b>
<b>3. MATERIALS AND METHODS</b> .....	<b>3</b>
<b>3.1. Materials</b> .....	<b>3</b>
3.1.1. Cell lines.....	3
3.1.2. Cell culture conditions.....	3
<b>3.5. Data mining</b> .....	<b>4</b>
<b>3.3. Cellular analysis. Cell growth curve</b> .....	<b>4</b>
<b>3.4. Molecular analysis</b> .....	<b>4</b>
3.4.1. Gene expression analysis.....	4
3.4.2. Protein expression analysis.....	5
<b>3.5. Statistical analysis</b> .....	<b>6</b>
<b>4. RESULTS</b> .....	<b>6</b>
<b>4.1. Cell growth at differential PGC1<math>\alpha</math> expression</b> .....	<b>6</b>
<b>4.2. Data mining</b> .....	<b>7</b>
<b>4.3. Cell cycle related PGC1<math>\alpha</math> transcriptional program</b> .....	<b>9</b>
<b>4.4. Protein expression. Rb phosphorylation under PGC1<math>\alpha</math> expression</b> .....	<b>9</b>
<b>4.5. Time course</b> .....	<b>10</b>
<b>5. DISCUSSION</b> .....	<b>11</b>
<b>6. CONCLUSION</b> .....	<b>13</b>
<b>7. REFERENCES</b> .....	<b>14</b>
<b>SUPPLEMENTARY DATA</b> .....	<b>i</b>

**Acknowledgements:** I want to thank Aroa and Ander for sharing this experience with me and for making it a lot more enjoyable. Thanks also to everyone in the laboratory, but especially to Alice for all her patience and for helping me throughout this time. Lastly, I want to thank Vero for giving me the opportunity to learn and grow in such a wonderful environment and for all her help.

## **1. INTRODUCTION**

Prostate cancer (PCa) is the second most common cancer in men, only behind lung cancer, with an estimated incidence of 990,345 cases worldwide in 2020<sup>1</sup>. Detection at an early stage relies essentially on prostate-specific antigen (PSA) presence in serum and digital rectal examination (DRE), followed by a trans-rectal biopsy if results show it to be necessary<sup>2</sup>. Primary treatment consists mainly of radical prostatectomy and radiotherapy, combined with androgen deprivation therapy (ADT) in more advanced conditions of the disease. Although PCa has a good prognosis and ADT reports favorable results in most cases, it can progress and reach a stage called Castration Resistant Prostate Cancer (CRPC) and develop metastasis<sup>3</sup>. Existing treatments for CRPC are palliative<sup>4</sup> and that is the reason why it is necessary to explore new strategies to address the disease. Regarding that issue, the development of precision medicine has become one of the main objectives in cancer and it seems increasingly crucial to find biomarkers that allow both to stratify patients and to propose a personalized treatment<sup>5</sup>.

Previous studies have described the transcriptional coactivator PPAR gamma co-activator 1 alpha (PGC1 $\alpha$ ) as a possible biomarker for the stratification of patients with PCa<sup>6</sup>. PGC1 $\alpha$  is a transcriptional coactivator that acts through different transcription factors or nuclear receptors, creating interactions across various N-terminal LXXLL leucine-rich motifs. It belongs to the PGC1 family and it is expressed mainly in tissues with a large number of mitochondria or that require a great oxidative metabolism, such as heart, skeletal muscle, brown adipose tissue, brain and kidney<sup>7</sup>. As PGC1 $\alpha$  is considered an essential modulator of cell metabolism, its implication in cancer has been studied over the past years.

Nonetheless, the role of the transcriptional coregulator PGC1 $\alpha$  in cancer is complex and it seems to be related to the context and tissue-specific characteristics. In the case of melanoma, the increased expression of PGC1 $\alpha$  is related to proliferation and survival; however, it reduces cells' invasive abilities. Accordingly, metastatic cells in melanoma cancer have a reduced expression of PGC1 $\alpha$ <sup>7</sup>. In breast cancer, PGC1 $\alpha$  also favors cell growth and proliferation and modulates the response to some treatments<sup>8</sup>. As well as in melanoma cells, in PCa PGC1 $\alpha$  has been observed to have anti-metastatic activity. It has also been proven its role in suppressing the proliferation of PCa cells, in addition to reducing anchorage-independent growth and burden tumor, something that did not occur in melanoma<sup>9,6</sup>.

As discussed above, PGC1 $\alpha$  performs its functions by interacting with different transcription factors, including ERR $\alpha$ . Estrogen-related receptor (ERR) is a family of ligand-activated transcription factors that have a C-terminal ligand-binding domain (LBD) to interact with PGC1 $\alpha$ , among others, and a zinc-finger DNA binding domain (DBD) to recognize and bind specific DNA sequences in order to carry out their functions as a transcription factor<sup>10</sup>. PGC1 $\alpha$ /ERR $\alpha$  transcriptional axis has been shown to be of great importance in cancer cells' metabolism, although its effect is, as mentioned earlier, dependent on the type of tumor<sup>11</sup>. In the specific case of PCa, PGC1 $\alpha$  operates in an ERR $\alpha$  dependent manner, thus controlling the invasive phenotype of cancer, as well as the proliferation, decreasing both of them<sup>9</sup>. In PCa cell lines, PGC1 $\alpha$  has also been reported to reduce the cell cycle progression and to arrest cells in G1 phase<sup>6</sup>.

However, despite PGC1 $\alpha$ 's role in the stratification of patients, it remains necessary to study its molecular mechanisms so that it can be targeted for personalized treatment. With that in mind, the laboratory performed an RNAseq of PCa cell lines with differential expression of PGC1 $\alpha$ . The preliminary data revealed more than 4,500 upregulated genes in the presence of PGC1 $\alpha$ , many of them related to oxidative metabolism and mitochondrial functions, as mentioned. In addition, it showed more than 3,000 downregulated genes, among which are some genes related to cell cycle, E2F and Myc target genes, for example.

Cell cycle (**Figure 1**) is regulated in several ways, one of the main ones being the phosphorylation/dephosphorylation of different proteins by cyclin/cyclin-dependent protein kinases (CDKs) complexes. These complexes act on cell cycle checkpoints and their objective is to control cell cycle progression from one phase to the next one<sup>12</sup>.

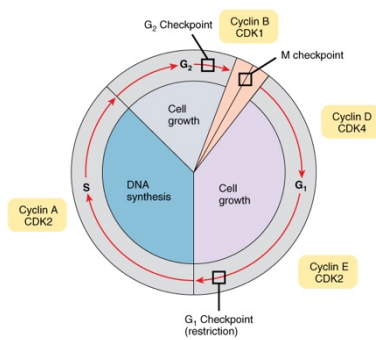


**Figure 1.** Cell cycle phases diagram. Checkpoints and cyclins and CDKs involved on each phase are represented. Source: OpenStax *Anatomy and Physiology*.

Retinoblastoma (Rb) protein is involved at several stages of the cell cycle but more specifically in the G1-to-S transition. This tumor suppressor is phosphorylated and dephosphorylated by diverse cyclin/CDK complexes; when dephosphorylated, Rb binds to the E2F transcription factor and remains bound as the cell enters G1 phase and it is mono-phosphorylated by cyclin D/CDK4-6 complex. Then, in late G1, Rb is multi-phosphorylated by cyclin E/CDK2 and consequently, the Rb/E2F complex dissociates<sup>13</sup>. E2F is a family of transcription factors that target MCM (minichromosome maintenance protein complex) genes, CDC6 or cyclins D and A among others, being closely associated with cell cycle progression and the transition to the DNA replication phase. When E2F interacts with Rb, the latter blocks the function of the E2F transcription factor and cells remain arrested in G1. Therefore, Rb phosphorylation at several residues is necessary for dissociation to occur and for E2F to fulfil its function<sup>14</sup>.

Cancer cells show an increased function of cyclin/CDK complexes and, in consequence, increased levels of Rb phosphorylation, resulting in deregulation of E2F function and uncontrolled proliferation, as mentioned above<sup>15</sup>. In addition, in PCa, proliferative androgen receptor (AR) signaling is known to be crucial for tumor development and survival<sup>16</sup>. AR is a nuclear transcription factor that affects E2F and Rb signaling in several ways, for example enhancing the expression of cyclin D and the formation of cyclin D/CDK4 complexes, which would lead, once again, to the phosphorylation of Rb and its loss of function as a repressor of E2F<sup>17</sup>.

## **2. HYPOTHESIS AND OBJECTIVES**

We have mentioned that coactivator PGC1 $\alpha$  has been shown to play an anti-proliferative role in PCa cells. Likewise, one of the characteristics of cancer is its uncontrolled cell proliferation due to cell cycle deregulation. Taking into account that preliminary information, we hypothesize that PGC1 $\alpha$  regulates the progression of the cycle and the G1-to-S phase transition targeting E2F transcriptional program. To this end, we aim to analyze: first, the transcriptional program associated with PGC1 $\alpha$  and related to cell cycle; second, the activity of CDK4 and associated proteins; and lastly, the correlations between PGC1 $\alpha$  and its transcriptional program in patients.

## **3. MATERIALS AND METHODS**

### **3.1. Materials.**

#### 3.1.1. Cell lines.

Human prostate carcinoma cell line PC3, which had been previously transduced with a modified TRIPZ doxycycline-inducible lentiviral construct containing mouse PGC1 $\alpha$  sequence (PC3 TRIPZ-HA-PGC1 $\alpha$ ), was used to perform all of the experiments.

#### 3.1.2. Cell culture conditions.

Cell lines were maintained using Dulbecco's Modified Eagle's Medium (DMEM) with glucose, L-glutamine, phenol red and no sodium pyruvate. DMEM was supplemented with 10% (v/v) inactivated Fetal Bovine Serum (FBS) and 1% (v/v) Penicillin-Streptomycin (complete medium).

Manipulation of cells was performed under sterile conditions in laminar flow cabinets. Cells were cultured in 100 mm dishes and incubated at 37 °C in 21% O<sub>2</sub> and 5% CO<sub>2</sub>. For preservation, cells were frozen in Dimethyl Sulfoxide (DMSO) 10% (v/v) in FBS solution at -80 °C after centrifugation (1200 rpm, 4 minutes, room temperature). On another note, fresh complete medium was added to cryovials for defrosting. As DMSO is toxic for cells and in order to prevent cells' death, the medium had to be changed the following day.

Routine cell passages were made every 3-4 days. For detaching, cells were washed with Dulbecco's Phosphate Buffered Saline (DPBS) (1X) and incubated for 3 minutes at 37 °C with 0.25% Trypsin-EDTA (1X) (Gibco) 1:4 DPBS dilution. DMEM was added to inactivate trypsin and resuspended cells were then diluted in complete media depending on initial confluence and seeded in a new plate.

To count cells, after the resuspension step, they were diluted 1:2 in 0.4% Trypan Blue Dye and counted in a Neubauer chamber using optical microscopy. Only death cells are blue-stained, as Trypan Blue Dye only enters the cytoplasm of cells whose membrane has been disrupted. That made possible to count viable (non-stained) cells.

0.5  $\mu$ g/mL of doxycycline hyclate (Dox) (Sigma #D9891) were used to induce PGC1 $\alpha$  expression in PC3 TRIPZ-HA-PGC1 $\alpha$  cells.

### **3.5. Data mining.**

The laboratory had previously performed an RNAseq with PGC1 $\alpha$  expressing cells (Dox) and non-expressing cells (No Dox). A functional enrichment of the PGC1 $\alpha$  expressing cells' upregulated and downregulated genes was performed using Cancertool<sup>18</sup>, focusing on Biocarta and Pathway enrichment types. In addition, Gene Set Enrichment Analysis (GSEA) was also used to carry out a complementary enrichment<sup>19</sup>. Both analyses were performed to determine the functions that were enriched in PGC1 $\alpha$  expressing condition (Dox). A group of genes that are included in the enriched cell function was selected for subsequent experiments.

Once candidate genes were chosen, Cancertool's "Correlations" feature was used to study correlation among that set of genes expression and PGC1 $\alpha$  on PCa patients.

### **3.3. Cellular analysis. Cell growth curve.**

Cell growth at differential PGC1 $\alpha$  expression conditions was analyzed. To induce PGC1 $\alpha$ , cell lines were pre-treated with dox. After 3 days, both doxycycline-treated and non-treated cells were resuspended, counted and seeded (10,000 cells/well) in technical triplicates with complete DMEM media in three 12-well-plates, corresponding to day 0, day 3 and day 6 of incubation.

Cells were fixed at day 0, day 3 and day 6 with formalin 10% after washing off non-adherent death cells with DPBS. Plates were stored at 4 °C until quantification. Crystal violet 0.1% (in 20% methanol) was used to stain attached cells, as it binds to DNA and proteins.

After shaking for 60 minutes, crystal violet was washed with distilled water, air-dried and resolubilized using 10% acetic acid for 1 hour. Resolubilized crystal violet was then transferred to a 96-well-plate to measure the absorbance (570 nm) using PowerWave XS Microplate Spectrophotometer (BioTek). The OD measured was directly proportional to the attached cell number and this allows to measure cell growth<sup>20</sup>.

### **3.4. Molecular analysis.**

#### **3.4.1. Gene expression analysis.**

As in growth analysis, doxycycline was used to pre-induce cells for three days before they were seeded (75,000 cells/well) in a 6-well-plate in a final volume of 2 mL in triplicate. Cells were incubated in DMEM for 3 days, then plates were frozen in liquid N<sub>2</sub> and stored at -80 °C after washing them with DPBS (1X). For time course experiment a different number of cells were seeded (400,000 cells/well) and were induced with doxycycline 2, 4, 6 or 8 hours before recollecting them.

RNA was extracted using NucleoSpin RNA isolation kit from Macherey-Nagel (ref: 740955.240C) following manufacture instructions and concentration was measured with a BioDrop spectrophotometer (Biochrom). To assess RNA purity, 260/280 nm and 260/230 nm ratios were considered; appropriate values are ~2.0 and ~2.0-2.2, respectively.

For cDNA synthesis, 1  $\mu$ g of RNA was mixed with 2  $\mu$ L of Thermo Scientific Maxima H Minus cDNA synthesis Master Mix (5X) and diluted up to 8  $\mu$ L with RNase-free water and. cDNA synthesis was performed

in a thermocycler at 25 °C for 10 minutes, at 50 °C for 15 minutes and lastly, at 85 °C for 5 minutes. The resulting cDNA product was diluted 1:9 in RNase-free water and stored.

For gene expression characterization, quantitative real-time PCR (qPCR) was performed using the Applied Biosystems QuantStudio 5 Real-Time PCR System (384-Well Block). CDC25A, CDK4, MCM7, E2F8 and MCM2 genes were analyzed using TaqMan technology, while MCM10, ORC1, WEE1, CDC7 and CDC45 genes were studied using SYBR Green technology. TaqMan assay relies on the use of gene-specific probes, besides gene-specific primers, consisting of a 3' quencher and a 5' reporter that release fluorescence when the gene is amplified. SYBR Green, on the other side, is a DNA intercalating agent that binds double strand DNA and emits more fluorescence than in solution. Therefore, as DNA is amplified using gene-specific primers, fluorescence emission increases, enabling us to measure the DNA product<sup>21</sup>.

For TaqMan amplified genes, 3 µL of TaqMan Universal Master Mix II, with UNG 2X (Applied Biosystems), forward and reverse primers (**Supplementary Table 1**) at a final concentration of 200 nM and gene-specific probes at a concentration of 100 nM were mixed and loaded to a 384-well-plate, before loading 3 µL of previously diluted cDNA (final volume = 6 µL). For SYBR Green, 3 µL of FastStart Universal SYBR Green Master (Roche) were mixed with forward and reverse primers (**Supplementary Table 1**) at a final concentration of 200 nM and loaded to the plate, so that 3 µL of cDNA could be added.

The following amplification program was used for TaqMan: 2 minutes at 50 °C, 10 minutes at 95 °C and, finally, 40 cycles of 15 seconds at 95 °C for denaturalization and 1 minute at 60 °C for annealing and elongation. For SYBR Green reaction the program was: 50 °C for 2 minutes and 95 °C for 10 minutes before 40 cycles of 95 °C for 15 seconds and 60 °C for 1 minute, to end with 95 °C for 15 seconds, 60 °C for 1 minute and 95 °C for other 15 minutes.

In both TaqMan and SYBR Green reactions, data obtained from amplified genes was normalized using a housekeeping gene, GAPDH in our case.

#### 3.4.2. Protein expression analysis.

For protein analysis, the same experimental setup as for RNA extraction was used (75,000 cells/well were seeded).

The plates were thawed in ice and cells' lysis was accomplished using 75 µL of RIPA lysis buffer (see **Supplementary Table 2**) per well. Cells were transferred to Eppendorf tubes and maintained on ice for 30 minutes, while vortexed every 4 minutes. After centrifugation (10 minutes, 14,000 g, 4 °C), supernatant was collected and transferred to new Eppendorf tubes. For protein quantification, Pierce<sup>TM</sup> BCA Protein Assay Kit (Thermo Fisher Scientific, ref: 23225) was used. First, we prepared a calibration curve with increasing concentrations of Bovine Serum Albumin (BSA) from 0.5 to 8 mg/mL. Samples were prepared by mixing 1 µL of the previously extracted protein with 9 µL of mili-Q water. BSA and samples were then loaded in duplicate to a 96-well-plate, 200 µL of BCA reagent was added to every well and the plate was incubated for 30 minutes at 37 °C afterwards. Absorbance was measured at 562 nm using PowerWave XS Microplate

Spectrophotometer (BioTek). Protein concentration was equalized in all samples by adding milli-Q water and Laemmli Loading Buffer 5X (see **Supplementary Table 3**).

In order to analyze proteins of interest, we performed a Western Blot. For that, samples were heated at 95 °C for 5 minutes and then subjected to SDS-PAGE, in which proteins were separated depending on their size. Both precast gels (Criterion™ XT Precast gels, 4-12% acrylamide, 12+2 well, BioRad) and homemade gels (resolving 7.5% and stacking 5% acrylamide, see **Supplementary Table 4**) were used. For each experiment and condition (Dox and No Dox) 15 µg (handmade gels) and 10 µg of protein (precast gels) were loaded in duplicate and Nippon MWP02 (DDBiolab) was used as a weight marker.

Electrophoresis was conducted in 1X Tris/Glycine/SDS running buffer at 90V for 15 minutes first and 150V for 1 hour afterwards in the case of homemade gels and in MOPS buffer at 180V for 90 minutes in the case of precast gels. In both homemade and precast gels, proteins were transferred to nitrocellulose membranes in transfer buffer 1X (10% transfer buffer 10X, composition in **Supplementary Table 5**, 20% ethanol, 70% milli-Q water) and the transference was carried out at 100V for 1 hour and 80V for 90 minutes, respectively. To assure that proteins were successfully transferred, membranes were stained with Ponceau S dye (0.1% (x/v) Ponceau S in 1% (v/v) acetic acid).

Before incubation with antibodies, membranes were blocked using 5% non-fat milk in Tris-Buffered Saline Solution with 0,01% Tween-20 (TBST) and washed also with TBST 1x. TBST with 0.002% sodium azide was used to prepare primary antibodies (the antibodies used are listed in **Supplementary Table 6**) at 1:1000 dilution, excluding  $\beta$ -actin, which was prepared at 1:2000. Membranes were incubated with primary antibodies overnight at 4 °C. For secondary antibody incubation, membranes were washed with TBST 1x and incubated for 1 hour at room temperature. Secondary antibodies were anti-rabbit (30111-035-144, Vitro s.a.) and anti-mouse (S30315-035-0454, Vitro s.a.) and were diluted 1:4000 in %5 non-fat milk in TBST. For membrane processing, Clarity™ Western ECL Substrate (Bio-Rad) and ChemiDoc Imaging System (Bio-Rad) were used.

GraphPad Prism 8 software was used for the statistical analysis of fold change relative to No Dox condition. One-sample t-test was performed, with a hypothetical value of 1 and confidence level of %95 ( $\alpha=0.05$ ).

### **3.5. Statistical analysis.**

GraphPad Prism 8 software was used for the statistical analysis of fold change relative to No Dox condition. One-sample t-test was performed, with a hypothetical value of 1 and confidence level of %95 ( $\alpha=0.05$ ). All experiments were repeated three times to ensure adequate statistical power.

## **4. RESULTS**

### **4.1. Cell growth at differential PGC1 $\alpha$ expression.**

Prior studies had shown that PGC1 $\alpha$  suppresses PCa growth. In order to confirm that our in vitro experimental system was performing well, proliferation under PGC1 $\alpha$ expressing (Dox) and non-expressing (No Dox) conditions was examined. As predicted, PGC1 $\alpha$  expressing cells showed a significantly decreased in cell



proliferation compared to non-expressing ones both at day 3 and day 6 (**Figure 2**). Taking into account previous laboratory experiments, the possibility that doxycycline treatment could affect the result was excluded<sup>6</sup>.

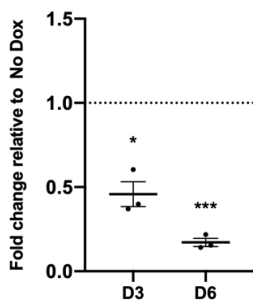


**Figure 2.** Cell growth at differential PGC1 $\alpha$  expression of PC3 TRIPZ-HA-PGC1 $\alpha$  cells. Cells were incubated for 3 and 6 days (N=3 independent experiments). Growth of Dox induced cells is represented relatively to No Dox condition (dotted line, value=1.0). D3=Day 3; D6=Day 6. Asterisk indicate statistical difference between 1.0 (No Dox) and Dox condition: \*\*\*,  $p < 0,001$ ; \*\*,  $p < 0,01$ ; \*,  $p < 0.05$ . Quantifications are presented as mean with SEM.

#### 4.2. Data mining.

As mentioned, the laboratory had performed an RNAseq with PGC1 $\alpha$  expressing and non-expressing cells and the results showed more than 4,500 upregulated and more than 3,000 downregulated genes in the presence of PGC1 $\alpha$ . We performed a functional enrichment analysis of that list of genes using Cancertool, focusing on those genes that appear downregulated in Dox condition, therefore being upregulated in No Dox condition. Different enrichment analysis were carried out by Cancertool, but we gave particular attention to *Biocarta* and *Pathway* (**Figure 3**).

On one side, *Biocarta* results show a significant downregulation of genes related to G2 cell cycle phase, in addition to MCM genes, which are as well related to cell cycle and mitosis. Furthermore, *Pathway* results reveal that cell cycle is the feature that is downregulated with the highest significance. Mitosis and mitosis related processes also appear to be downregulated in Dox condition, according to the information obtained from the enrichment.

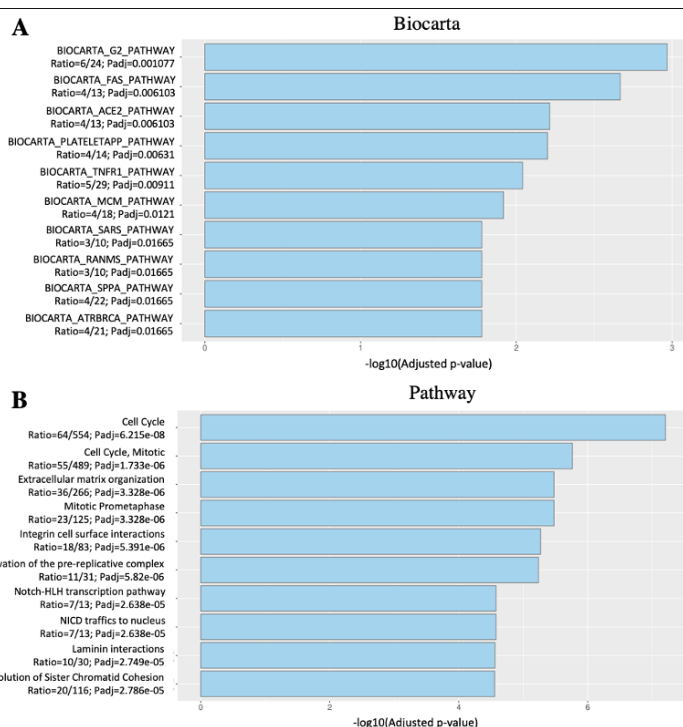


**Figure 3.** Functional enrichment analysis results provided by Cancertool. The ten terms with the highest significance according to adjusted p-value are shown. A) Biocarta enrichment and B) Pathway enrichment. The X-axis indicates the  $-\log_{10}$  of the adjusted p-value and the Y-axis contains information about the category, the ratio (count/size, size being the number of genes assigned to the category and count the gene count from the provide list that correspond to the category) and the adjusted p-value (Padj)<sup>18</sup>.

Next, we performed an additional enrichment using GSEA. We found that gene sets that are enriched in PC3 cells without PGC1 $\alpha$  expression (No Dox condition), that is, aggressive cells, are mainly E2F targets and Myc targets (**Figure 4**). Myc is a target gene of PGC1 $\alpha$  (referencia) and E2F targets are associated with cell cycle and cell cycle progression.

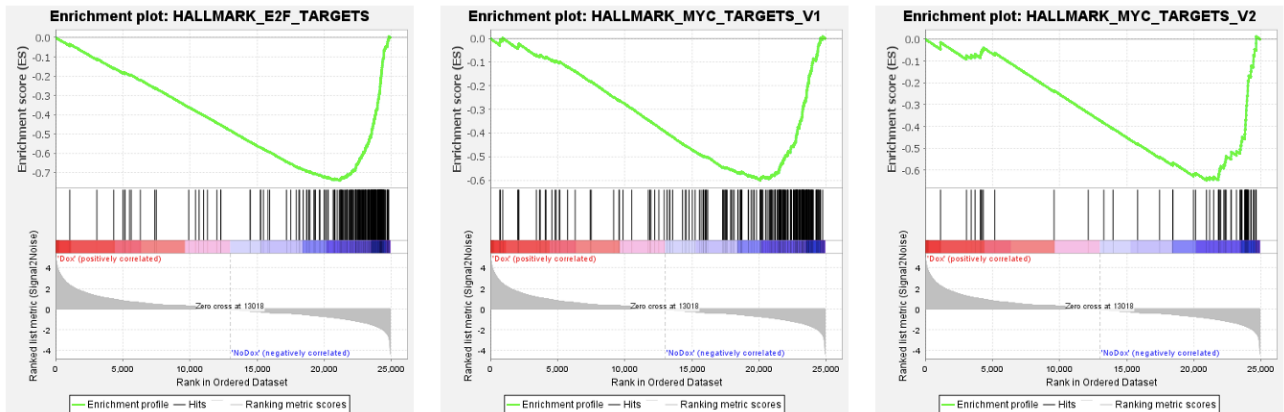


**Figure 4.** Functional enrichment analysis results for E2F and Myc targets provided by GSEA. The enrichment score (ES) on the X-axis reflects the degree to which a gene set is overrepresented at the top or bottom of a ranked list of genes. The negative ES indicates gene set enrichment at the bottom of the ranked list at No Dox condition (blue region, Dox condition being red region)<sup>19</sup>. NES (Normalized Enrichment Score) values from left to right are -3.62, -2.85 and -2.58. FDR (False Discovery Rate) q-value is the estimated probability that a gene set with a given NES represents a false positive finding. The values from left to right are 0.000, 0.000 and 0.000.

Taking into account the information obtained from functional enrichment and bibliographic research, 11 genes which appear downregulated on PGC1 $\alpha$  expressing cells (Dox condition) were selected for further analyses, all of them being related to cell cycle: CDC6, CDC25A, MCM10, MCM2, MCM7, CDK4, ORC1, E2F8, WEE1, CDC7 and CDC45. Using Cancertool, we studied gene expression correlation between PGC1 $\alpha$  and all the candidate genes in PCa patient datasets (**Figure 5**).

No consistency	(*) R = -0.235 p = 0.0369	R = 0.118 p = 0.424	R = -0.187 p = 0.541	(*) R = -0.405 p = 2e-06	(*) R = -0.454 p < 2.2e-16	R = -0.083 p = 0.673	R = -0.607 p = 0.167	CDK4
No consistency	R = -0.215 p = 0.0568	(*) R = -0.403 p = 0.00484	R = -0.159 p = 0.604	R = -0.03 p = 0.729	(*) R = -0.422 p = 1.01e-22	R = -0.07 p = 0.729	R = -0.286 p = 0.556	CDC6
No consistency	R = 0.144 p = 0.204	(*) R = -0.295 p = 0.0461	R = 0.038 p = 0.906	R = -0.032 p = 0.72	(*) R = -0.252 p = 1.43e-08	R = 0.094 p = 0.669	R = 0 p = 1	CDC25A
No consistency	R = -0.016 p = 0.886	R = -0.148 p = 0.315	R = -0.121 p = 0.696	R = -0.176 p = 0.0448	R = -0.12 p = 0.00775	R = -0.317 p = 0.41	R = -0.321 p = 0.498	WEE1
No consistency	R = -0.201 p = 0.0739	R = 0.122 p = 0.408	R = -0.297 p = 0.525	R = 0.06 p = 0.494	R = -0.06 p = 0.16	R = -0.196 p = 0.38	R = 0.071 p = 0.906	CDC7
No consistency	R = 0.058 p = 0.611	(*) R = -0.322 p = 0.0276	NA	R = 0.058 p = 0.51	NA	R = -0.383 p = 0.0752	(*) R = 0.786 p = 0.046	ORC1
No consistency	R = -0.024 p = 0.833	R = -0.146 p = 0.32	R = -0.055 p = 0.663	R = -0.051 p = 0.563	(*) R = -0.314 p = 9.01e-13	R = -0.078 p = 0.693	R = 0.143 p = 0.783	MCM2
No consistency	R = -0.202 p = 0.0742	(*) R = -0.298 p = 0.0399	R = 0.111 p = 0.723	(*) R = -0.372 p = 1.39e-05	(*) R = -0.366 p = 2.34e-17	NA	R = 0.286 p = 0.556	MCM7
No consistency	R = 0.101 p = 0.378	R = -0.329 p = 0.182	NA	R = 0.035 p = 0.69	(*) R = -0.361 p = 1.4e-16	NA	R = 0.143 p = 0.783	MCM10
No consistency	(*) R = -0.345 p = 0.00183	R = -0.068 p = 0.686	R = -0.516 p = 0.074	R = 0.029 p = 0.746	R = -0.178 p = 7.25e-05	R = 0.233 p = 0.335	R = -0.357 p = 0.444	E2F8
	Glinisky	Grasso	Lapointe	Taylor	TCGA	Tomlins	Varambally	

**Figure 5.** Heatmat provided by Cancertool for correlation between PGC1 $\alpha$  and the genes on the right in multiple datasets. Red color shade indicates a direct correlation (correlation coefficient toward 1) and blue color shade indicates an inverse correlation (correlation coefficient toward -1). Correlations on concrete datasets are indicated with asterisks following the criteria:  $p \leq 0.05$  and Spearman correlation coefficient greater than 0.2 or lower than -0.2 for direct or inverse correlations, respectively. On the left side, the coherence among data sets is shown for each pair of genes (significant correlation in more than 50% of datasets)<sup>18</sup>.

While none of the candidate genes shows significant correlation in more than 50% of datasets (consistency), CDK4 and MCM7 show significance in Taylor and TCGA (The Cancer Genome Atlas) cohorts, besides exhibiting solid correlation also in Glinsky and Grasso datasets, respectively. The number of PCa patients in those datasets is larger and the clinical data is better characterized<sup>18</sup>.

#### **4.3. Cell cycle related PGC1 $\alpha$ transcriptional program.**

Considering the information obtained from data mining and functional enrichment analyses, we next performed a gene expression profiling of PGC1 $\alpha$  expressing (Dox) and non-expressing (No Dox) PC3 cell lines. In order to validate that candidate genes were downregulated in PGC1 $\alpha$  expressing cells, as it was previously observed in the RNAseq analysis, various qPCR were carried out. As we had predicted, all of the genes had a reduced expression in Dox induced condition (**Figure 6**). CDC6 gene expression could not be analyzed since TaqMan probe and/or primers did not work as expected and the gene could not be amplified nor measured.

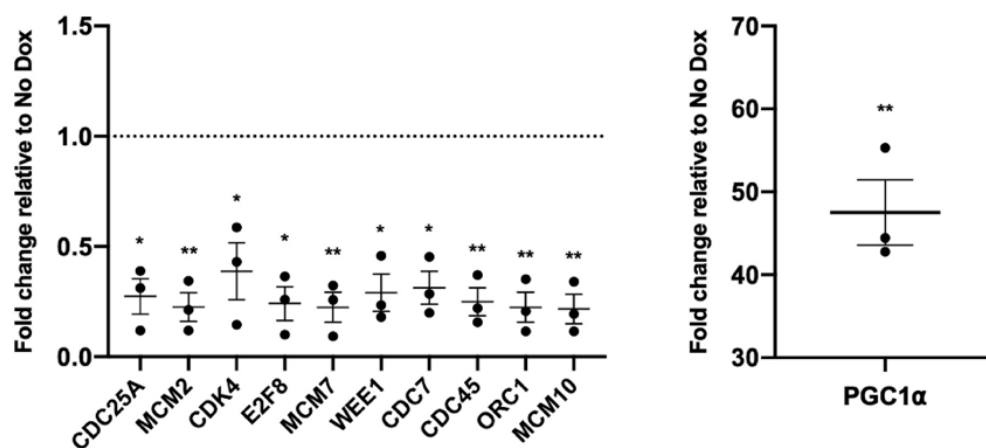


**Figure 6.** mRNA Expression of candidate genes (left panel) and PGC1 $\alpha$  (right panel) in PC3 TRIPZ-HA-PGC1 $\alpha$  cells incubated for 3+3 days. (N=3 independent experiments). Expression in Dox induced cells is represented relatively to No Dox condition (dotted line, value=1.0). Asterisk indicate statistical difference between 1.0 (No Dox) and Dox condition: \*\*\*, p < 0,001; \*\*, p < 0,01; \*, p < 0.05. Quantifications are presented as mean with SEM.

#### **4.4. Protein expression. Rb phosphorylation under PGC1 $\alpha$ expression.**

As data mining pointed that CDK4 was a gene of interest, was validated by qPCR and knowing from literature that it is involved in Rb phosphorylation and cell cycle progression, we considered analyzing protein expression and Rb phosphorylation in PC3 cell line. PGC1 $\alpha$ -expressing (Dox) and non-expressing (No Dox) cells' expression of CDK4, cyclin D1 and total Rb, as well as phospho-Rb were compared and the results are displayed in **Figure 7**.

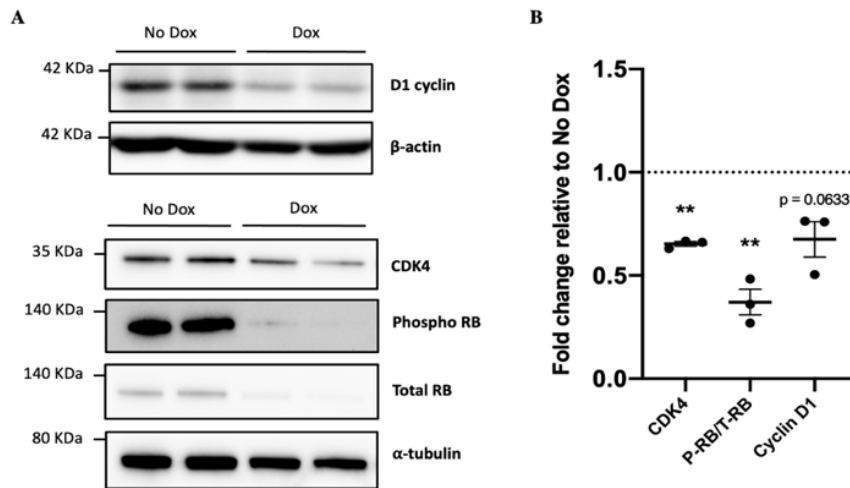


**Figure 7.** Effect of PGC1 $\alpha$  expression in CDK4, cyclin D1 and Rb protein expression, in addition to Rb phosphorylation in Ser780 residue. A) Representative Western Blot results out of three experiments. Experiments were performed in PC3 TRIPZ-HA-PGC1 $\alpha$  cells incubated for 3+3 days. (N=3 independent experiments). B) Quantification of the protein expression level. Expression in Dox induced cells is represented relatively to No Dox condition (dotted line, value=1.0). Asterisk indicate statistical difference between 1.0 (No Dox) and Dox condition: \*\*\*, p < 0,001; \*\*, p < 0,01; \*, p < 0.05. Quantifications are presented as mean with SEM.

CDK4 shows a significant decrease of expression in PGC1 $\alpha$  presence. Although cyclin D1, with which CDK4 works on Rb mono-phosphorylation, does not reach confidence level, it also shows a reduction compared to No Dox condition. In addition, phospho-Rb/total-Rb ratio appears decreased in PGC1 $\alpha$  expressing cells, therefore showing a decreased phosphorylation of Rb protein. As can be noted in the left panel of **Figure 7**, besides the reduction in Rb phosphorylation, total-Rb protein expression also reveals a reduction in Dox condition, that is to say, under PGC1 $\alpha$  expression. The results corroborate that PGC1 $\alpha$  impacts not only on both CDK4 gene and protein expression, but also on Rb phosphorylation and total Rb, molecular events that could affect cell cycle progression.

#### **4.5. Time course.**

To further characterize the dynamics of transcriptional regulation of some of the selected genes(MCM10, MCM7 and CDK4) by PGC1 $\alpha$ , a short doxycycline time course was carried out. Given the notion that cell cycle related genes are generally regulated by the oncogene Myc and that our lab has previously described that PGC1 $\alpha$  transcriptionally represses the Myc in a time dependent manner, we wonder if the changes in our candidate genes were downstream of Myc canonical repression triggered by PGC1 $\alpha$ . The gene expression of the selected genes was monitor upon PGC1 $\alpha$  induction at 2, 4, 6 and 8 hours of treatment with doxycyclinep. Results show a significant reduction of the expression of MCM10 at 8 hours, although all of the genes exhibit a tendency to reduce their expression after the first 6 hours (**Figure 8**). Considering those results, it would be useful to determine additional time points in order to monitor the beginning of the decrease in the expression. It would also be necessary to perform some complementary experiments to ensure that Myc mediates MCM10, CDK4 and MCM7 expression.

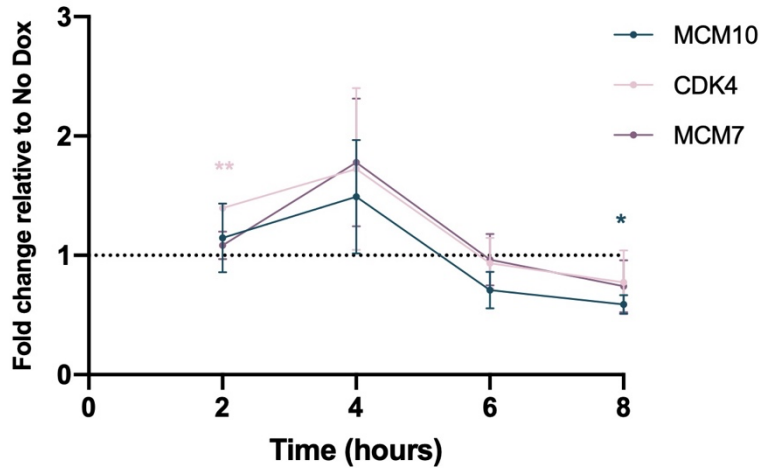


**Figure 8.** Gene expression analysis of CDK4, MCM7 and MCM10 at 2, 4, 6 and 8 hours of doxycline induction and PGC1 $\alpha$  expression (N=3 independent experiments). Expression in Dox induced cells is represented relatively to No Dox condition (dotted line, value=1.0). Asterisk indicate statistical difference between 1.0 (No Dox) and Dox condition (blue for MCM10 and pink for CDK4): \*\*\*,  $p < 0,001$ ; \*\*,  $p < 0,01$ ; \*,  $p < 0.05$ .

## 5. DISCUSSION

PGC1 $\alpha$ , through ERR $\alpha$ , has been demonstrated to reduce cell proliferation in PCa, besides preventing tumor dissemination and metastasis<sup>6,9</sup>. We confirmed that proliferative reduction of cancer cells elicited by PGC1 $\alpha$  was also happening in PC3TRIPZ-HA-PGC1 $\alpha$  cell line we were using for the subsequent experiments, as expected from previous studies.

As mentioned, the laboratory had previously performed an RNAseq, obtaining more than 7000 genes either upregulated or downregulated in PGC1 $\alpha$  presence. Functional enrichments of RNAseq data revealed that cell cycle is one of the main pathways downregulated in PGC1 $\alpha$  expressing cells, thus being enriched in non-expressing aggressive cells. Cancer is characterized by increased and uncontrolled cell proliferation, partly due to a signaling cascade that affects G1-to-S and G2-to-M transitions<sup>12</sup>; therefore, the results of RNAseq data enrichments are consistent and coherent with published information and what is described about cancer and cancer cells' behavior.

Analyzing those cell cycle-related genes, which appear downregulated in PGC1 $\alpha$  expressing cells, is of great relevance because it means that they appear upregulated in cells that do not express PGC1 $\alpha$  and, therefore, exhibit a more aggressive phenotype. That is, it would serve to identify possible therapeutic targets associated with PGC1 $\alpha$  expression. Taking into account the literature and the information of the RNAseq and pertinent enrichments, we studied the transcriptional program associated with the cell cycle in PCa PC3 cell line, both in PGC1 $\alpha$  expressing and non-expressing conditions. All of the candidate genes present a strong relation with different cell cycle processes and showed reduced expression in the case of induced cells, as predicted since it was described that PGC1 $\alpha$  arrested cells in G1 phase<sup>6</sup>. To assure that PGC1 $\alpha$  plays a role in cell cycle by conditioning the transcription of associated genes it would be convenient to make a rescue experiment of those genes in PGC1 $\alpha$ -expressing cells and observe if proliferation is reduced and cells remain arrested in G1 phase.

As in the functional enrichment performed by GSEA, we observed that E2F and Myc target genes were enriched under PGC1 $\alpha$  expression, we raised the possibility that Myc was mediating the effect of PGC1 $\alpha$  in

the cell cycle. With that in mind, a short time course of the expression of three of the candidate genes was carried out. Even though results showed a significant decrease only in the case of MCM10, we can appreciate that the genes exhibit a reduction at 6 and 8 hours. Considering that previous studies have shown a significant repression of Myc expression within the first 2 hours after induction of PGC1 $\alpha$  expression<sup>9</sup>, it could be suggested that Myc mediated the expression of cell cycle-related genes. Those results would be in line with the knowledge of that Myc affects CDK4, among others, contributing to cell cycle deregulation in cancer cells<sup>22,23</sup>. In order to verify that hypothesis in our cells, it would be interesting to study the expression of the time course genes in Myc knock out cells (shMyc cells) or, what is more, to make a rescue experiment of Myc in the PC3 TRIPZ-HA-PGC1 $\alpha$  cells after the induction of PGC1 $\alpha$ .

Once we had confirmed that the inducible PGC1 $\alpha$  expression system was working, as we could see in the growth curve, we focused on studying CDK4 and the Rb phosphorylation/dephosphorylation axis, since CDK4 appear in the RNAseq and its kinase activity is of great importance in the alteration of the cell cycle in cancer<sup>24</sup>. As mentioned, CDK4 expression is decreased in both the RNAseq and the qPCR. We wanted to check if, besides the gene expression, CDK4 activity was also compromised in PGC1 $\alpha$  expressing cells. Besides results showing that CDK4 protein expression is reduced, the ratio of phosphorylated Rb compared to the total Rb is decreased in cells expressing PGC1 $\alpha$ , hence being increased in aggressive PGC1 $\alpha$ -non-expressing cells. This is consistent with the previous studies describing a deregulation of CDK4 activity in a wide variety of tumors, in which CDK4 exhibits a higher activity and therefore, Rb phosphorylation-rate is elevated<sup>25</sup>. As mentioned, Rb phosphorylation is necessary for cell cycle progression, since that way Rb dissociates from E2F, leading to cell cycle-related genes transcription<sup>14</sup>.

However, even though Rb does not appear decreased under PGC1 $\alpha$  in the RNAseq data, the total amount of Rb does appear reduced in the protein analysis, in addition to the reduction of the phosphorylation. The same happens in the case of cyclin D1, so we can speculate that in both cases the decrease occur at protein translation level, protein stability or both. In any case, the results are consistent with the prediction: in PGC1 $\alpha$  expressing cells, important cell cycle related genes are reduced, as Rb phosphorylation is crucial for G1-to-S phase transition<sup>26</sup>. Moreover, correlations carried out by Cancertool showed an inverse relationship between PGC1 $\alpha$  and CDK4 in three of the seven datasets, as we could observe in the provided heatmap.

Targeting the Rb phosphorylation process mediated by cyclin D/CDK4-6 complex may be a promising therapeutic strategy for treating PCa, once PGC1 $\alpha$  expression in the patient was monitored. This could lead to the use of PGC1 $\alpha$  as a biomarker for personalized medicine, besides its function in stratifying patients with low and high expression, as previously proposed<sup>6</sup>. In breast cancer, cyclin-dependent kinases are already being the target of several commercialized drugs: palbociclib, ribociclib and abemaciclib. All three are CDK4/6 inhibitors and have been shown to be highly effective in treating different subtypes of breast cancer, in combination with endocrine therapy<sup>27</sup>.

Nonetheless, in PCa, results are quite disappointing so far. For example, flavoripidol, a CDK inhibitor that had previously shown clinical efficacy in xenografts, did not achieve the expectations in a phase II trial of metastatic hormone-refractory PCa<sup>28</sup>. A similar situation was described with palbociclib in the treatment of

Rb-expressing metastatic hormone-sensitive PCa. Palbociclib had good preclinical results but did not demonstrate its efficacy in a phase II trial<sup>29</sup>. Focusing on CRPC, there are currently some clinical trials to demonstrate the efficacy of different CDK4/6 inhibitors (NCT02494921 o NCT02905318), including the already mentioned palbociclib, in the treatment of CRPC<sup>30</sup>. However, it should be taken into account that metastatic castration-resistant prostate cancers had shown a high heterogeneity of Rb expression since, among multiple options, loss of Rb both at genomics and protein level may occur, due to Rb deletions, among others<sup>31</sup>. In those cases, targeting CDK4/6, which would lead to reduced Rb phosphorylation, may not have the expected results, as those patients would not have experienced hyperphosphorylation of Rb. Moreover, PGC1 $\alpha$  expression should be taking into account when it comes to consider clinical trials' results. Knowing that PGC1 $\alpha$  decreases Rb phosphorylation, as demonstrated in the Western Blot analysis, those patients with high PGC1 $\alpha$  expression may not respond to the inhibition of CDK4 for the reason that they already had low phospho-Rb. Meanwhile, patients with low PGC1 $\alpha$  expression might show better results as their Rb phosphorylation is increased, compared to those whose PGC1 $\alpha$  level is much higher.

Considering this heterogeneity, in breast cancer loss of Rb has been proposed as a biomarker to anticipate the results of the treatment against CDK4/6<sup>32</sup>. It would be an option to use it in the same way with PCa if studies prove it to be effective..

## **6. CONCLUSION.**

To summarize, our results suggest that the effect PGC1 $\alpha$ /ERR $\alpha$  axis has on cell cycle progression in PCa is mediated by Rb/E2F axis and cyclin D/CDK4-6 phosphorylation of Rb. That could lead to a better knowledge of PGC1 $\alpha$ 's molecular mechanisms and could point to CDK4 as a potential target for personalized therapy in prostate cancer, taking into account the role of PGC1 $\alpha$  in patients' stratification.

## **7. REFERENCES**

1. Cancer Today. Accessed May 21, 2021. [https://gco.iarc.fr/today/online-analysis-multi-bars?v=2020&mode=cancer&mode\\_population=countries&population=900&populations=900&key=asr&sex=1&cancer=39&type=0&statistic=5&prevalence=0&population\\_group=0&ages\\_group%5B%5D=0&ages\\_group%5B%5D=17&nb\\_items=10&](https://gco.iarc.fr/today/online-analysis-multi-bars?v=2020&mode=cancer&mode_population=countries&population=900&populations=900&key=asr&sex=1&cancer=39&type=0&statistic=5&prevalence=0&population_group=0&ages_group%5B%5D=0&ages_group%5B%5D=17&nb_items=10&)
2. Borley N, Feneley MR. Prostate cancer: diagnosis and staging. *Asian J Androl.* 2009;11(1):74-80. doi:10.1038/aja.2008.19
3. Jaiswal S, Sarmad R, Arora S, Dasaraju R, Sarmad K. Prostate Cancer for the Internist. *N Am J Med Sci.* 2015;7(10):429-435. doi:10.4103/1947-2714.168660
4. Mansinho A, Macedo D, Fernandes I, Costa L. Castration-Resistant Prostate Cancer: Mechanisms, Targets and Treatment BT - Molecular & Diagnostic Imaging in Prostate Cancer: Clinical Applications and Treatment Strategies. In: Schatten H, ed. Springer International Publishing; 2018:117-133. doi:10.1007/978-3-319-99286-0\_7
5. Mateo J, McKay R, Abida W, et al. Accelerating precision medicine in metastatic prostate cancer. *Nat Cancer.* 2020;1(11):1041-1053. doi:10.1038/s43018-020-00141-0
6. Torrano V, Valcarcel-Jimenez L, Cortazar AR, et al. The metabolic co-regulator PGC1 $\alpha$  suppresses prostate cancer metastasis. *Nat Cell Biol.* 2016;18(6):645-656. doi:10.1038/ncb3357
7. Bost F, Kaminski L. The metabolic modulator PGC-1 $\alpha$  in cancer. *Am J Cancer Res.* 2019;9(2):198-211. <https://pubmed.ncbi.nlm.nih.gov/30906622>
8. Andrzejewski S, Klimcakova E, Johnson RM, et al. PGC-1 $\alpha$  Promotes Breast Cancer Metastasis and Confers Bioenergetic Flexibility against Metabolic Drugs. *Cell Metab.* 2017;26(5):778-787.e5. doi:<https://doi.org/10.1016/j.cmet.2017.09.006>
9. Valcarcel-Jimenez L, Macchia A, Crosas-Molist E, et al. PGC1 $\alpha$  Suppresses Prostate Cancer Cell Invasion through ERR $\alpha$  Transcriptional Control. *Cancer Res.* 2019;79(24):6153-6165. doi:10.1158/0008-5472.CAN-19-1231
10. Villena JA, Kralli A. ERR $\alpha$ : a metabolic function for the oldest orphan. *Trends Endocrinol Metab.* 2008;19(8):269-276. doi:10.1016/j.tem.2008.07.005
11. Deblois G, St-Pierre J, Giguère V. The PGC-1/ERR signaling axis in cancer. *Oncogene.* 2013;32(30):3483-3490. doi:10.1038/onc.2012.529
12. Collins I, Garrett MD. Targeting the cell division cycle in cancer: CDK and cell cycle checkpoint kinase inhibitors. *Curr Opin Pharmacol.* 2005;5(4):366-373. doi:<https://doi.org/10.1016/j.coph.2005.04.009>
13. Fischer M, Müller GA. Cell cycle transcription control: DREAM/MuvB and RB-E2F complexes. *Crit Rev Biochem Mol Biol.* 2017;52(6):638-662. doi:10.1080/10409238.2017.1360836
14. Li Y, Barbash O, Diehl JA. Regulation of the Cell Cycle. In: *The Molecular Basis of Cancer: Fourth Edition.* Elsevier Inc.; 2015:165-178.e2. doi:10.1016/B978-1-4557-4066-6.00011-1
15. Burke JR, Deshong AJ, Pelton JG, Rubin SM. Phosphorylation-induced Conformational Changes in the Retinoblastoma Protein Inhibit E2F Transactivation Domain Binding \*. *J Biol Chem.* 2010;285(21):16286-16293. doi:10.1074/jbc.M110.108167
16. Crumbaker M, Khoja L, Joshua AM. AR Signaling and the PI3K Pathway in Prostate Cancer. *Cancers (Basel).* 2017;9(4):34. doi:10.3390/cancers9040034
17. Burkhardt DL, Morel KL, Sheahan A V, Richards ZA, Ellis L. The Role of RB in Prostate Cancer Progression. In: Dehm SM, Tindall DJ, eds. *Prostate Cancer: Cellular and Genetic Mechanisms of Disease Development and Progression.* Springer International Publishing; 2019:301-318. doi:10.1007/978-3-030-32656-2\_13
18. Cortazar AR, Torrano V, Martín-Martín N, et al. CANCERTOOL: A Visualization and Representation Interface to Exploit Cancer Datasets. *Cancer Res.* 2018;78(21):6320-6328. doi:10.1158/0008-5472.CAN-18-1669
19. Subramanian A, Tamayo P, Mootha VK, et al. Gene set enrichment analysis: A knowledge-based approach for interpreting genome-wide expression profiles. *Proc*



- Natl Acad Sci.* 2005;102(43):15545 LP - 15550.  
doi:10.1073/pnas.0506580102
20. Feoktistova M, Geserick P, Leverkus M. Crystal Violet Assay for Determining Viability of Cultured Cells. *Cold Spring Harb Protoc.* 2016;2016(4):pdb.prot087379.  
doi:10.1101/pdb.prot087379
21. Tajadini M, Panjehpour M, Javanmard SH. Comparison of SYBR Green and TaqMan methods in quantitative real-time polymerase chain reaction analysis of four adenosine receptor subtypes. *Adv Biomed Res.* 2014;3:85. doi:10.4103/2277-9175.127998
22. Hermeking H, Rago C, Schuhmacher M, et al. Identification of CDK4 as a target of c-MYC. *Proc Natl Acad Sci U S A.* 2000;97(5):2229-2234.  
doi:10.1073/pnas.050586197
23. Mateyak MK, Obaya AJ, Sedivy JM. c-Myc regulates cyclin D-Cdk4 and -Cdk6 activity but affects cell cycle progression at multiple independent points. *Mol Cell Biol.* 1999;19(7):4672-4683.  
doi:10.1128/MCB.19.7.4672
24. Narasimha AM, Kaulich M, Shapiro GS, Choi YJ, Sicinski P, Dowdy SF. Cyclin D activates the Rb tumor suppressor by mono-phosphorylation. *Elife.* 2014;3.  
doi:10.7554/eLife.02872
25. Goel S, DeCristo MJ, McAllister SS, Zhao JJ. CDK4/6 Inhibition in Cancer: Beyond Cell Cycle Arrest. *Trends Cell Biol.* 2018;28(11):911-925.  
doi:https://doi.org/10.1016/j.tcb.2018.07.002
26. Topacio BR, Zatulovskiy E, Cristea S, et al. Cyclin D-Cdk4,6 Drives Cell-Cycle Progression via the Retinoblastoma Protein's C-Terminal Helix. *Mol Cell.* 2019;74(4):758-770.e4.  
doi:10.1016/j.molcel.2019.03.020
27. Gao JJ, Cheng J, Bloomquist E, et al. CDK4/6 inhibitor treatment for patients with hormone receptor-positive, HER2-negative, advanced or metastatic breast cancer: a US Food and Drug Administration pooled analysis. *Lancet Oncol.* 2020;21(2):250-260.  
doi:https://doi.org/10.1016/S1470-2045(19)30804-6
28. Liu G, Gandara DR, Lara PN, et al. A Phase II Trial of Flavopiridol (NSC #649890) in Patients with Previously Untreated Metastatic Androgen-Independent Prostate Cancer. *Clin Cancer Res.* 2004;10(3):924-928.  
doi:10.1158/1078-0432.CCR-03-0050
29. Palmboos PL, Daignault-Newton S, Tomlins SA, et al. A Randomized Phase II Study of Androgen Deprivation Therapy with or without Palbociclib in RB-positive Metastatic Hormone-Sensitive Prostate Cancer. *Clin Cancer Res.* 2021;27(11):3017-3027.  
doi:10.1158/1078-0432.CCR-21-0024
30. Batra A, Winkquist E. Emerging cell cycle inhibitors for treating metastatic castration-resistant prostate cancer. *Expert Opin Emerg Drugs.* 2018;23(4):271-282.  
doi:10.1080/14728214.2018.1547707
31. Rodrigues D, Casiraghi N, Romanel A, et al. RB1 Heterogeneity in Advanced Metastatic Castration Resistant Prostate Cancer. *Clin Cancer Res.* 2018;25:clincanres.2068.2018. doi:10.1158/1078-0432.CCR-18-2068
32. Malorni L, Piazza S, Ciani Y, et al. A gene expression signature of retinoblastoma loss-of-function is a predictive biomarker of resistance to palbociclib in breast cancer cell lines and is prognostic in patients with ER positive early breast cancer. *Oncotarget.* 2016;7(42):68012-68022.  
doi:10.18632/oncotarget.12010

## **SUPPLEMENTARY DATA**

**Supplementary Table 1.** Information about the primer sequences used for TaqMan and SYBR Green amplification.

<b>Gene</b>	<b>Species</b>	<b>Forward primer (5' - 3')</b>	<b>Reverse primer (5' - 3')</b>
CDC25A	Human	CGTCATGAGAACTACAAACCTTGA	TCTGGTCTCTTCAACACTGACC
CDK4	Human	GTGCAGTCGGTGGTACCTG	AGGCAGAGATTCGCTTGTGT
MCM7	Human	GATCCTGGTGTGGCCAAG	CCCGGCCTGTTGTGTACT
E2F8	Human	AATGACATCTGCCTTGACGA	GTAAATGCGTCGACGTTCAA
MCM2	Human	CGAAACCTGGTTGTTGCTG	GGTGAAGGATTCCGATGATTC
MCM10	Human	CCCAACCCCTACAGACGATT	TTCGGCCGGTCATTTTCTTG
ORC1	Human	AGAGATCTTCAGTGGTGCCA	GCTGCTGCCTAATCCGATTC
WEE1	Human	TCGATATTTCTCTGCGTGGG	GGCCAACTTGCAAAGGAGA
CDC7	Human	TGAACTTCAGTGCCTAACAGT	GACTCATGCTCCAGATATGGC
CDC45	Human	CAGGGATGAAGAGGAGGATGA	GGTTTGCTCCACTATCTCCTC

**Supplementary Table 2.** RIPA lysis buffer (Roche) composition.

<b>RIPA lysis buffer</b>	
TrisHCl pH 7.5, 50 mM	1% Sodium deoxycholate
NaCl, 150 mM	Sodium fluoride, 1 mM
EDTA, 1mM	Sodium orthovanadate, 1 mM
0.1% SDS	Betaglycerophosphate, 1mM
1% Nonidet P40	Protease inhibitor cocktail

**Supplementary Table 3.** Laemmli protein loading buffer composition.

<b>Laemmli loading buffer 5X</b>	
10% SDS	1% $\beta$ -mercaptoethanol
Tris pH 6.8, 50 mM	DTT, 10 mM
10% H <sub>2</sub> O	0.2 mg/mL Bromophenol blue
50% Glycerol	

**Supplementary Table 4.** Homemade acrylamide gels recipe.

	<b>Resolving gel 7.5% acrylamide</b>	<b>Stacking gel 5% acrylamide</b>
<b>30% Acrylamide</b>	7.5%	5%
<b>Tris (1.5 M, pH 8.8)</b>	25%	25%
<b>10% SDS</b>	1%	1%
<b>10% APS</b>	1%	1%
<b>TEMED</b>	0.04%	0.04%
<b>Milli-Q water</b>	Up to final volume	Up to final volume

**Supplementary Table 5.** Western Blot transfer buffer composition.

<b>Transfer buffer 10X</b>	
Glycine, 200 mM	Tris, 25 mM

**Supplementary Table 6.** Information about the antibodies used for protein detection.

<b>Protein</b>	<b>Isotype</b>	<b>Reference</b>	<b>Commercial house</b>
Rb	Mouse IgG	9309	Cell Signaling Technology
CDK4	Rabbit IgG	12790	Cell Signaling Technology
Phospho-Rb	Mouse IgG	9307	Cell Signaling Technology
B-actin	Mouse IgG	3700	Cell Signaling Technology
Cyclin D1	Mouse IgG	SC-8396 HRP	Santa Cruz Biotechnology
$\alpha$ -tubulin	Mouse IgG	T9026	Sigma-Aldrich